Optimization on photoelectric detection based on stacked $La_{0.9}Sr_{0.1}MnO_{3-\delta}/LaAlO_{3-\delta}$ multijunctions

Jie Xing,[1,a)] Hui Ying Hao,[1] Er Jia Guo,[2] and Fang Yang[2]
[1]*School of Materials Sciences and Technology, China University of Geosciences, Beijing 100083, China*
[2]*Beijing National Laboratory for Condensed Matter Physics, Institute of Physics, Chinese Academy of Science, Beijing 100190, China*

(Received 12 May 2011; accepted 29 June 2011; published online 3 August 2011)

Three multijunctions consisting of $La_{0.9}Sr_{0.1}MnO_{3-\delta}$ and $LaAlO_{3-\delta}$ on Si substrate have been fabricated under different oxygen pressures by laser molecular beam epitaxy. They exhibit nonlinear and rectifying current-voltage characteristics and evident photocurrent response to He-Ne laser illumination. Experimental results indicate that the periodically stacked multijunction grown under lower oxygen pressure shows a better rectification behavior and a higher photocurrent. The photovoltaic responsivities of the multijunctions are enhanced greatly at reverse bias and are much higher than that of a similarly grown single p-n junction. Based on the band structure of the multilayers, a possible mechanism of the photovoltaic process was proposed. A high photovoltage responsivity of 168.6 mV/mW has been achieved at -6 V bias; this demonstrates the potential of the present multijunction configuration for photodetectors operating at room temperature. © *2011 American Institute of Physics*. [doi:10.1063/1.3621143]

I. INTRODUCTION

Perovskite oxides have been an important class of materials due to their abundant dielectric, piezoelectric, ferroelectric, ferromagnetic, optical, and superconducting properties.[1–6] Since the first perovskite p-n junction was created in 1999, lots of perovskite based p-n junctions have been fabricated following by the various experimental and theoretical works around the physics underlying the rich and extraordinary phenomena. Extensive efforts have been devoted to the dependence of electric transport properties of a single heterojunction on the temperature, magnetic field, electric field, and light.[7–11] Recently, a lot of research activity has been attracted by the enhanced functionalities based on multilayer structure, for example, ferroelectricity with large dielectric constant,[12] strong magnetoelectric coupling,[13] large magnetoresistance,[14,15] high carrier mobility, and conductivity at heterointerface.[16] Our previous work has been concentrated on studying the physical characteristics of a single p-n cell, including ultrafast and high sensitive photovoltaic effects in $La_{0.7}Sr_{0.3}MnO_3$/Si, $LaAlO_{3-\delta}$/Si, $BaTiO_{3-\delta}$/Si, and $La_{0.9}Sr_{0.1}MnO_3/SrNb_{0.01}Ti_{0.99}O_3$ heterojunctions, etc.[17–20] However, the optical characteristics of a stacked multijunction structure have remained relatively unexplored.[21,22] In this letter, we investigate the electrical and photovoltaic properties of a series of stacked p-n junctions composed of $La_{0.9}Sr_{0.1}MnO_{3-\delta}$ and $LaAlO_{3-\delta}$ films on Si substrate and study the oxygen pressure dependence of these physical properties.

II. EXPERIMENTAL DETAILS

The multilayers of $La_{0.9}Sr_{0.1}MnO_{3-\delta}$ (LSMO)/$LaAlO_{3-\delta}$ (LAO) were epitaxially grown on n-type Si (001) substrate by a computer-controlled laser molecular beam epitaxy system. First, a 100-nm-thick p-type LSMO was deposited onto Si substrate to form the first p-n junction. Then, two 10-nm-thick LAO and two 100-nm-thick LSMO were stacked alternatively on the LSMO-coated Si substrate as shown in the left inset of Fig. 1. Three samples were named SH, SM, and SL corresponding to their deposition oxygen pressure of 1×10^{-2}, 1×10^{-3}, and 1×10^{-4} Pa, respectively. Details about the deposition procedure can be found elsewhere.[15] Sharp and bright reflective high-energy electron diffraction patterns showed that the films were all epitaxially grown on the Si substrates. A typical x-ray diffraction pattern is shown in the right inset of Fig. 1. Except for (00*l*) diffraction peaks of LSMO and Si, there are no diffraction peaks from impurity phases or randomly oriented grains. As the LAO film is only 10 nm thick, no evident diffraction peak from LAO layer could be detected. Current-voltage measurement was carried out by using a Keithley 2400 sourcemeter. The photoelectric properties were investigated by using a 632.8 nm He-Ne laser with a power density of 1 mW/mm^2, and the signals were recorded by a 500 MHz digital oscilloscope with an input impedance of 1 MΩ.

III. RESULTS AND DISCUSSIONS

Figure 1 shows the current-voltage (*I-V*) characteristics of the three samples measured in darkness at room temperature. The forward direction is defined as the current flowing from LSMO film to Si substrate (Fig. 1, left inset). All the three samples display typical rectification behaviors. There is also some significant difference among them. For the sample SL grown under the lowest oxygen pressure (10^{-4} Pa), the forward current rises quickly with bias while the reverse current is smaller than that of the other two samples. The current ratio of sample SL at ± 2 V is about 200. To further understand the conduction mechanism, we have

[a)]Author to whom correspondence should be addressed. Electronic mail: jxing2011@gmail.com.

 © 2011 American Institute of Physics

Downloaded 03 Aug 2011 to 147.8.171.167. Redistribution subject to AIP license or copyright; see http://jap.aip.org/about/rights_and_permissions

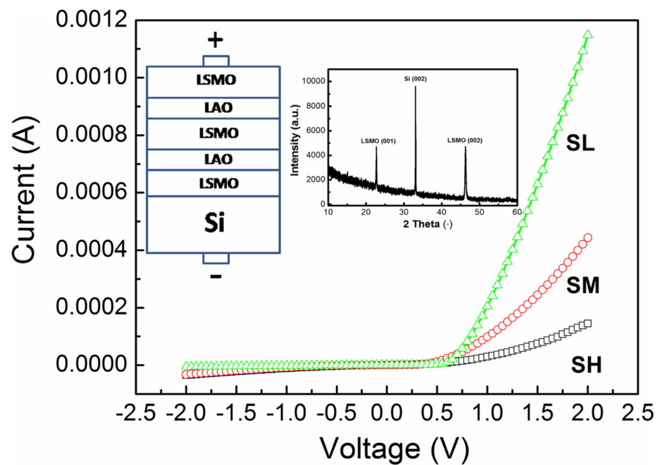

FIG. 1. (Color online) The current-voltage characteristics of samples SL, SM, and SH in darkness at room temperature. The left inset shows a schematic illustration of the sample measurement. The right inset shows a typical XRD pattern of samples.

replotted the positive branches of *I-V* curves in a double-logarithmic scale as shown in Fig. 2. The slope for each segment of the curves, i.e. (d(logI)/d(logV)), is labeled near the curves. At low applied voltage, the *I-V* characteristics of the three samples approximately follow Ohm's law because the density of thermally generated free carriers inside the films is predominant over that of injected charge carriers. When the bias reaches up to a threshold voltage V_T, the injected excess carriers dominate the thermally generated carriers, and a transition from ohmic to space-charge-limited (SCL) conduction occurs in the *I-V* curves. Among the three samples, the slope of sample SH changes most slowly. When the voltage sweeps from 0.05 V to 2 V, the slope changes smoothly from 1 to 2. SCL conduction with no traps can be described by Child's law $J = 9\varepsilon_0\varepsilon_r\mu V^2/8d^3$, in which ε_0 is the permittivity of free space, ε_r the static dielectric constant, μ the mobility, and V the applied voltage.[23] So the conduction mechanism in sample SH between 0.5 V and 2 V is dominated by SCL conduction with no traps. For sample SM, the current rises rapidly at the voltage of 0.25 V with a slope of 4. And for sample SL, the slope changes from 0.5 to 6 at 0.5 V. The region with higher slope (>2) in *I-V* curves of sample SM and SL is corresponding to a trap-filled limit (TFL) region, which indicates the existence of oxygen vacancies-related trap levels distributed in the bandgap. When the bias voltage exceeds V_T, the electrons in the traps will obtain enough activation energy to jump over the trap barrier, and the empty trap will be refilled by the newly injected carriers. The trapping-based conduction process is considered as TFL conduction. Eventually, when all the existing trapping centers are occupied by the injected carriers, the slope reduces gradually. Then the conduction mode transforms into trap-free space charge conduction, which obeys Child's law. For the three samples, an evident shoulder-like feature appears in the *I-V* curve of SL as is more easily seen in Fig. 3. This specific transport behavior comes from the abrupt transition of conduction modes from ohmic to TFL conduction. Due to the existence of a large number of oxygen vacancies levels in SL distributed exponentially in the bandgap,[24] the slope of *I-V* curve in the TFL region is significantly higher than those of the other two samples. The abrupt change of slope brings about a shoulder-like feature.

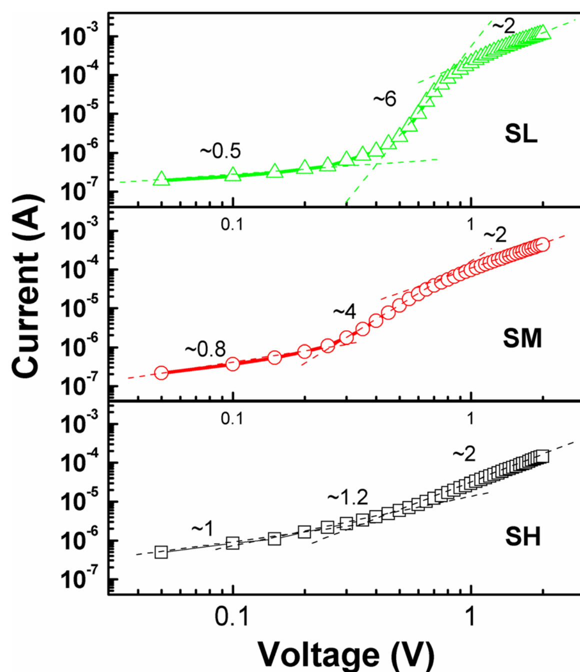

FIG. 2. (Color online) The positive branches of current-voltage curves of samples SL, SM, and SH in a double-logarithmic scale.

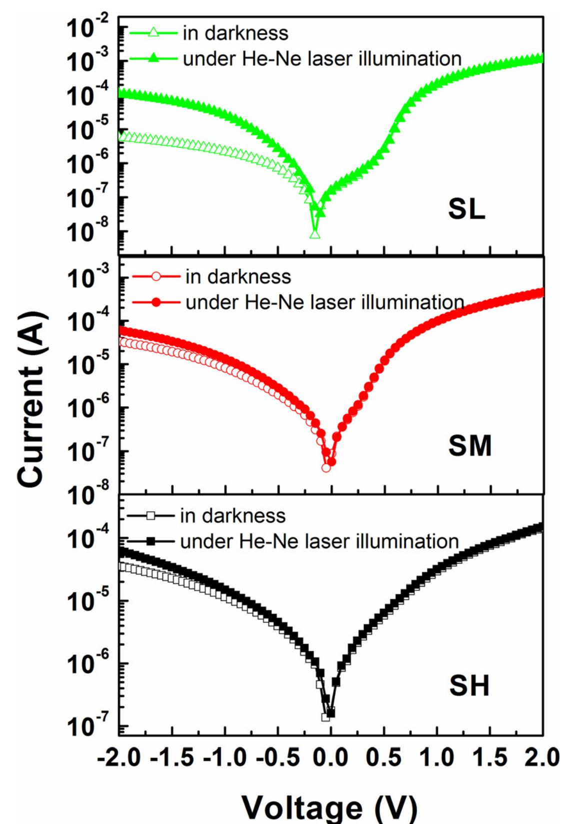

FIG. 3. (Color online) The current-voltage curves of samples SL, SM, and SH in semi-logarithmic scale under He-Ne laser illumination and in darkness.

Downloaded 03 Aug 2011 to 147.8.171.167. Redistribution subject to AIP license or copyright; see http://jap.aip.org/about/rights_and_permissions

As we stated in the preceding text, all the three samples have multi-layers with LSMO-LAO-LSMO-LAO-LSMO-Si in sequence. LSMO is a p-type semiconductor. Stoichiometric $LaAlO_3$ is an insulator; however, its electrical conduction can be significantly enhanced when grown in an oxygen-poor environment because each oxygen vacancy can donate two extra electrons. Thus the n-type LAO film has a higher electron density but lower hole density than LSMO. Then the electrons in LAO will diffuse into LSMO, and the holes in LSMO will diffuse into LAO. Such diffusion constructs a built-in electric field in the space charge region around the interface. The overall electrical transport behavior of the multijunction in series is determined by the accumulated transport asymmetry of each constituent single p-n cell.

Figure 3 shows the *I-V* curves of the three samples under He-Ne laser illumination in semi-logarithmic scale plot at room temperature. For comparison, the *I-V* curves measured in darkness are also added in this figure. The open and solid symbols denote the data measured in darkness and under illumination, respectively. It is clear that a sizable photocurrent appears at reverse bias and the photocurrent increases with the reverse biased voltage. The photocurrent change with bias of sample SH, SM, and SL show a similar tendency. However, at the same bias, the photocurrent of SL is the biggest and that of SH is the smallest; this indicates that the multijunction grown under the lower oxygen pressure has a higher photocurrent response.

As is well known, the heating effect due to illumination maybe causes the current change. To clarify the origin of the photocurrent, we took a CO_2 laser with wavelength of 10.6 μm to illuminate the three samples. Yet no evident current changes were observed for the three samples. The photon energy of CO_2 laser is 0.12 eV, which is smaller than the bandgaps of LSMO and Si. That means no carriers can be excited by photo-absorption. However, the heating effect due to illumination with such an infrared laser is unavoidable. No evident current changes were measured during illumination, which manifests that heating-induced current is small and can be almost neglected.

To further investigate their photovoltaic properties, we used a He-Ne laser and an oscilloscope to measure the photovoltages directly. Taking sample SL as an example, when the laser spot is incident onto the film perpendicularly, the open-circuit photovoltage of the sample is only 64 mV. But at -4 V bias, the photovoltage can reach up to 760 mV as displayed in Fig. 4. The much enhanced photovoltage at reverse bias is a result of multijunction stacked structure. Our sample is a p-n-p-n-p-n multijunction, which has three single p-n cells connected in series. This kind of configuration inevitably leads to formation of an inversely oriented heterojunction between the donor layer of the front cell and the acceptor layer of the following back cell. As shown in Fig. 5(a), when the multijunction is under irradiation, LSMO and Si will absorb photons to generate electrons and holes. Electrons in the conduction band of LSMO, driven by the built-in field at interface, will drift into the conduction band of Si (or LAO) on the left side and that of LAO on the right side. The opposite movement of electrons will largely weaken the net photocurrent and lead to accumulation of electrons in the LAO layer. So, the photovoltage at no bias is small due to the counteracting effect of adjacent cells. To prevent carriers' pile-up at the inverse p-n cell, an external reverse bias is applied to the multijunction as shown in Fig. 5(b). The bias can effectively enhance the built-in field at p-n interface and depress it at n-p interface. Thus, photogenerated carriers can be efficiently transferred across multi-interface and collected at the electrodes. Hence, the photovoltage is much enhanced at reverse bias.

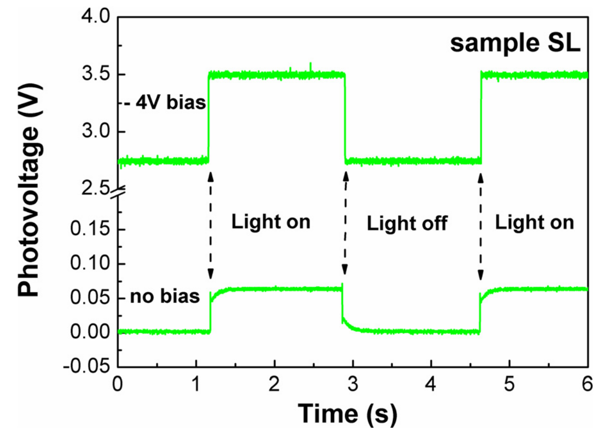

FIG. 4. (Color online) Variation of the photovoltage of sample SL with time at no bias and at -4 V bias, respectively, under He-Ne illumination.

Figure 6 gives the dependence of photovoltage responsivity R_V on reverse bias for the three samples, where R_V is defined as photovoltage divided by on-sample power. We can see that photovoltages for the three samples are all enhanced with the increased bias. The R_Vs of sample SL, SM, and SH are 168.6, 43.1, and 19.0 mV/mW, respectively, at -6 V bias compared with 9.14, 1.54, and 1.02 mV/mW at 0 bias. Sample SL shows the highest photovoltages, which is in agreement with the result of the *I-V* measurement.

In the inset of Fig. 6 is the variation of R_V for sample SH at zero bias with time, recorded directly by oscilloscope. It can be found that an up-side (down-side) spike appears when the He-Ne laser is switched on (off). However, the

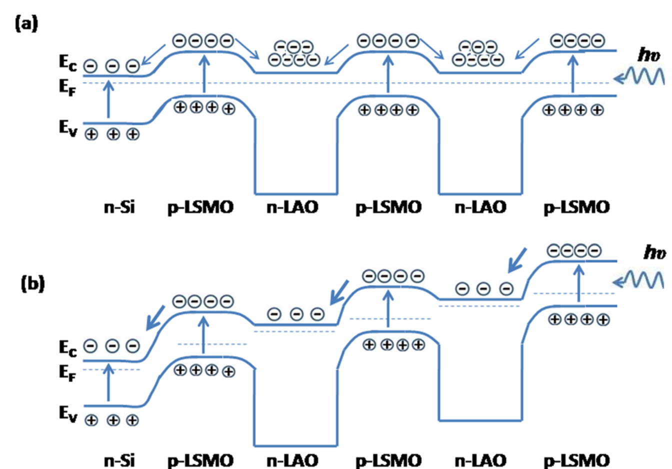

FIG. 5. (Color online) The schematic band structure of the LSMO-LAO-LSMO-LAO-LSMO-Si multijunction under illumination at (a) no bias and (b) reverse bias. E_C, E_F, and E_V denote the conduction band level, Fermi level, and valence band level, respectively.

Downloaded 03 Aug 2011 to 147.8.171.167. Redistribution subject to AIP license or copyright; see http://jap.aip.org/about/rights_and_permissions

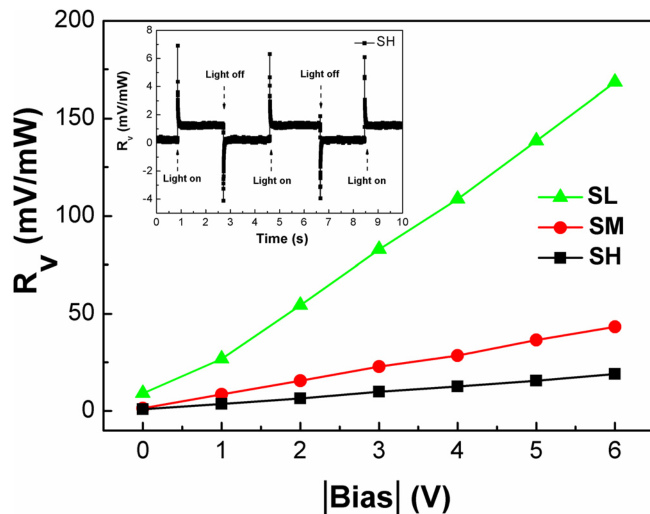

FIG. 6. (Color online) The photovoltage responsivity of sample SL, SM, and SH vs reverse bias. Inset is a photovoltage responsivity at zero bias of sample SH recorded by an oscilloscope.

open-circuit photovoltage of sample SL (shown in Fig. 4) has not such a feature at all. The similar phenomena has ever been observed in $LaAlO_{3-\delta}$/Si and $BaTiO_{3-\delta}$/Si heterojunctions.[18,19] We conjecture it may be related with oxygen vacancies in samples. Sample SL and SH are prepared under the oxygen pressure of 10^{-4} Pa and 10^{-2} Pa respectively, so SL has much more oxygen vacancies than SH. The oxygen vacancies are trap centers that could trap photo-generated electrons and deter their recombination with holes. Thus the lifetime of photocarriers in SL is much longer than that in SH. In sample SH, many photo-induced holes and electrons, due to their short lifetime, have recombined quickly upon generation. In the inset of Fig. 6, the spikes just manifest a generating and recombining process from holes and electrons in sample SH. However, in SL, because of the longer carriers' lifetime, the photo-generated holes and electrons are effectively separated by the built-in field and collected at electrodes before recombination. Therefore, there is no spike presenting in the photovoltage measurement. And so, we can understand the photoresponse of SL is higher than that of SM, and SM is higher than SH.

The photovoltage responsivity of sample SH at zero bias is about 1.02 mV/mW, which is the lowest among the three samples but still six times that of ~0.17 mV/mW obtained in a similarly grown $La_{0.9}Sr_{0.1}MnO_3$/Si single junction in our previous work.[25] It indicates that such a stacked multijunction is an effective configuration to improve the photovoltage responsivity. To achieve higher photoelectric conversion efficiency, not only the photovoltage but also the photocurrent in the multijunction should be considered. Further optimization, such as designing the thickness of every layer and careful balancing the photocurrent of each cell, is currently in progress.

IV. SUMMARY

In conclusion, we have prepared three multijunctions based on stacking $La_{0.9}Sr_{0.1}MnO_{3-\delta}$ and $LaAlO_{3-\delta}$ alternatively on Si substrates under different oxygen pressures. It is found that the multijunction grown under lower oxygen pressure has a better rectification behavior and a higher photocurrent. And at reverse bias, the photocurrents/photovoltages are enhanced greatly due to the efficient transfer of carriers across the multi-interface. A high photovoltage responsivity of 168.6 mV/mW has been achieved at -6 V bias, which manifests that the present optimized stacked p-n junction has great potential prospect in photodetection.

ACKNOWLEDGMENTS

This work is supported by the National Natural Science Foundation of China, Fundamental Research Funds for the Central Universities (Grant Nos. 2010ZY50 and 2011YYL006), Open Research Fund Program of National Laboratory of Mineral Materials of China University of Geosciences and Open Research Fund Program of Key Laboratory of Optical Physics, Institute of Physics, Chinese Academy of Sciences.

[1]C. Wang, B. L. Cheng, S. Y. Wang, H. B. Lu, Y. L. Zhou, Z. H. Cheng, and G. Z. Yang, Appl. Phys. Lett. **84**, 765 (2004).
[2]A-M. Haghiri-Gosnet and J-P. Renard, J. Phys. D **36**, R127 (2003).
[3]G. Liu and C. W. Nan, J. Phys. D **38**, 584 (2005).
[4]R. R. Jia, J. C. Zhang, R. K. Zheng, D. M. Deng, H.-U. Habermeier, H. L. W. Chan, H. S. Luo, and S. X. Cao, Phys. Rev. B **82**, 104418 (2010).
[5]S. Mathews, R. Ramesh, T. Venkatesan, and J. Benedetto, Science **276**, 238 (1997).
[6]J. Gao and F. X. Hu, Mater. Sci. Eng. B **126**, 250 (2006).
[7]K. J. Jin, H. B. Lu, K. Zhao, C. Ge, M. He, and G. Z. Yang, Adv. Mater. **21**, 4636 (2009).
[8]K. J. Jin, H. B. Lu, Q. L. Zhou, K. Zhao, B. L. Cheng, Z. H. Chen, Y. L. Zhou, and G. Z. Yang, Phys. Rev. B **71**, 184428 (2005).
[9]H. Tanaka, J. Zhang, and T. Kawai, Phys. Rev. Lett. **88**, 027204 (2002).
[10]A. D. Wei, J. R. Sun, W. M. Lu, and B. G. Shen, Appl. Phys. Lett. **95**, 052502 (2009).
[11]Z. G. Sheng, Y. P. Sun, X. B. Zhu, J. M. Dai, W. H. Song, Z. R. Yang, L. Hu, and R. R. Zhang, J. Phys. D **41**, 135008 (2008).
[12]E. Bousquet, M. Dawber, N. Stucki, C. Lichtensteiger, P. Hermet, S. Gariglio, J.-M Triscone, and P. Ghosez, Nature **452**, 732 (2008).
[13]Y. Tokura, J. Magn. Magn. Mater. **310**, 1145 (2007).
[14]H. B. Lu, G. Z. Yang, Z. H. Chen, S. Y. Dai, Y. L. Zhou, K. J. Jin, B. L. Cheng, M. He, L. F. Liu, H. Z. Guo, Y. Y. Fei, W. F. Xiang, and L. Yan, Appl. Phys. Lett. **84**, 5007 (2004).
[15]K. Zhao, K. J. Jin, H. B. Lu, M. He, Y. H. Huang, G. Z. Yang, and J. D. Zhang, Appl. Phys. Lett. **93**, 252110 (2008).
[16]J. Son, J. M. LeBeau, A. S. James, and S. Stemmer, Appl. Phys. Lett. **97**, 202109 (2010).
[17]H. B. Lu, K. J. Jin, Y. H. Huang, M. He, K. Zhao, B. L. Cheng, Z. H. Chen, Y. L. Zhou, S. Y. Dai, and G. Z. Yang, Appl. Phys. Lett. **86**, 241915 (2004).
[18]J. Xing, K. J. Jin, H. B. Lu, M. He, G. Z. Yang, J. Qiu, and G. Z. Yang, Appl. Phys. Lett. **92**, 071113 (2008).
[19]J. Xing, E. J. Guo and J. Wen, Chin. Phys. B **20**, 037304 (2011).
[20]J. Qiu, H. B. Lu, K. J. Jin, M. He, and J. Xing, Physica B **400**, 66 (2007).
[21]H. Liu, K. Zhao, N. Zhou, H. B. Lu, M. He, Y. H. Huang, K. J. Jin, Y. L. Zhou, G. Z. Yang, S. Q. Zhao, A. J. Wang, and W. X. Leng, Appl. Phys. Lett. **93**, 171911 (2008).
[22]N. Zhou, K. Zhao, H. Liu, H.B Lu, M. He, S. Q. Zhao, W. X. Leng, A. J. Wang, Y. H. Huang, K. J. Jin, Y. L. Zhou, and G. Z. Yang, J. Phys. D **41**, 155414 (2008).
[23]K. C. Kao and W. Hwang, *Electrical Transport in Solids* (Pergamon, Oxford, 1981).
[24]D. S. Shang, Q. Wang, L. D. Chen, R. Dong, X. M. Li, and W. Q. Zhang, Phys. Rev. B **73**, 245427 (2006).
[25]J. Xing, K. Zhao, G. Z. Liu, M. He, K. J. Jin, and H. B. Lu, J. Phys. D **40**, 5892 (2007).

Downloaded 03 Aug 2011 to 147.8.171.167. Redistribution subject to AIP license or copyright; see http://jap.aip.org/about/rights_and_permissions